

## Planar Gold Nanoparticle Clusters as Microscale Mirrors

Jin Young Kim and Frank E. Osterloh\*

Department of Chemistry, University of California, Davis, One Shields Avenue, Davis, California 95616

Received November 22, 2005; E-mail: fosterloh@ucdavis.edu

The ability to manipulate light over small length scales is the basis for many areas of technology, including communications, displays, and spectroscopy. Miniaturized mirrors, which are among the simplest waveguiding devices, are employed in spatial light modulators,<sup>1,2</sup> in optical switches,<sup>3,4</sup> and as light-emitting devices in commercial projection displays.<sup>5</sup> Virtually all micromirrors are fabricated lithographically from metal-coated or uncoated silicon.<sup>1,4,5</sup> In extension of our work on nanoparticle-based waveguides,<sup>6–9</sup> we report here a scalable *chemical* synthesis of micrometer-scale mirrors based on Au nanoparticles and  $\text{Ca}_2\text{Nb}_3\text{O}_{10}$  nanoplates. Similar to their macroscale analogues, these *nanoparticle mirrors* (NMs) are capable of directional light reflection. Because of their small size, these NMs can be dispersed in polar and nonpolar solvents, potentially allowing uses as optical probes to investigate the flow of liquids, or as fillers for polymers with tailored optical properties.

Micromirror plates are produced as shown in Figure 1a (experimental details in Supporting Information). Reaction of  $\text{Ca}_2\text{Nb}_3\text{O}_{10}$  nanoplates with 3-aminopropyltrimethoxysilane produces 3-aminopropylsilyl-modified perovskite plates as described earlier.<sup>7</sup> Addition of a suspension of the perovskite colloid to an aqueous dispersion of  $12.3 \pm 0.9$  nm citrate-coated gold nanoparticles produces NMs of type **1**. In these NMs, monolayers of gold nanoparticles are bonded to both sides of the perovskite plates via N–Au interactions. Through alternating reactions with 1,8-octanedithiol followed by treatment with citrate-coated gold nanoparticles, it is possible to increase the thickness of the gold layers. This produces NMs of types **2** and **3**. TEM images of NMs (Figure 1b) reveal increasing gold nanoparticle densities from  $3180 \pm 110$  per  $\mu\text{m}^2$  for type **1** to  $12\,700 \pm 750$  per  $\mu\text{m}^2$  for type **3** NMs. The thickness of the NMs increases accordingly from  $72 \pm 25$  nm (type **1**) to  $114 \pm 25$  nm (type **2**) and  $139 \pm 35$  nm (type **3**). Expectedly, the lateral dimensions of the NMs ( $1.3 \pm 0.4$   $\mu\text{m}$ ) are independent of the number of nanoparticle layers.

Dispersions of the NMs in organic solvents appear dark due to a broad absorption band in the 500–800 nm region (Figure 2a) that is shifted to increasingly longer wavelength with increasing gold nanoparticle density. Synchronous scan emission spectra reveal that the absorbance at 600–800 nm is mostly due to light scattering. Because of their larger volume, the NMs prove to be stronger Mie scatterers than the  $\text{Ca}_2\text{Nb}_3\text{O}_{10}$  or Au nanoparticle precursors (Figure 2b). The decrease of scattering intensity  $I_S$  at  $\lambda > 800$  nm can be understood in terms of scattering theory which predicts  $I_S \sim \lambda^{-4}$ .<sup>10</sup>

Using a laser light source, it can be shown that the nanoparticle mirrors scatter light in a directional way, that is, they behave like mirrors. Figure 2c shows optical micrographs (10X objective, NA = 0.25, reflected light) of a few hundred type **3** NMs on a glass substrate under illumination with a mercury light source and a laser light source (654 nm) pointing at the sample at 30° vertical angle (see inset in Figure 2c). Even though the entire sample is illuminated by laser light, only a few particles appear red. The fact that the bright red spots have the same size as the plates suggests that light

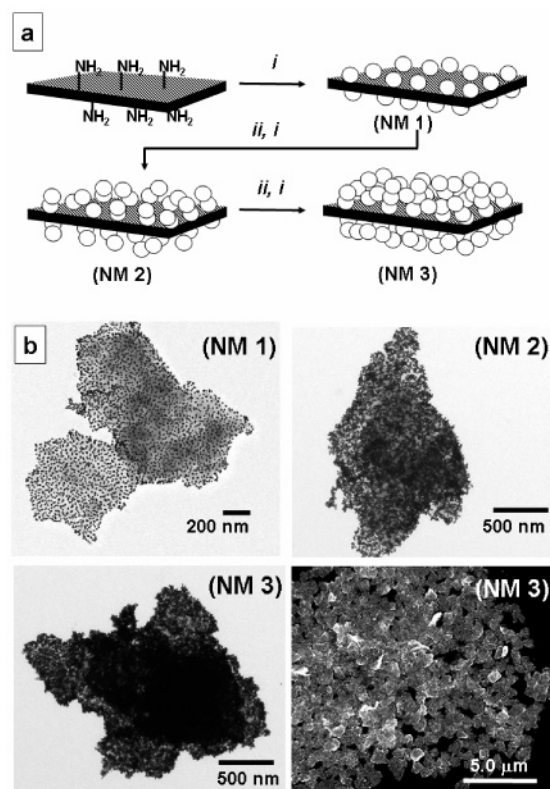


**Figure 1.** (a) Synthesis of mirror plates. For detailed structure of amine-terminated nanoplates, see ref 7. (i) Citrate-coated gold nanoparticles in water:ethanol (1:1 v/v), followed by centrifugation; (ii) 1,8-octanedithiol in ethanol. (b) Transmission electron micrographs of types **1–3** NMs and scanning electron micrograph of a few hundred type **3** NMs (additional SEMs are shown on page S-3).

intensity originates from individual particles in the sample and is due to light reflection. Accordingly, by changing the horizontal angle of the incident light, it is possible to observe reflection from a different set of particles. By inserting a polarizing filter between sample and detector, it is also possible to show that laser light reflected by the particles retains the polarization of the incident light (S-4 in Supporting Information). This demonstrates that the gold plate particles do not behave like isotropic Mie scatterers, whose emission is nondirectional and nonpolarized (for a demonstration with ZnO microcrystals, see S-5 in Supporting Information). The directional light reflection properties are also apparent in the bright field micrograph in Figure 2e. Here, only particles with their planes perpendicular to the viewing direction appear bright, whereas the rest of the sample is dark due to nonreflective particle orientations. Type **3** nanoparticle mirrors dispersed in ethanol/glycerol under illumination by two separate lasers ( $\lambda_1 = 654$  nm,  $\lambda_2 = 532$  nm) at 180° horizontal angle display Brownian motion-driven multicolor blinking behavior (images in Figure 2d; movie in Supporting Information). Depending on their steadily changing

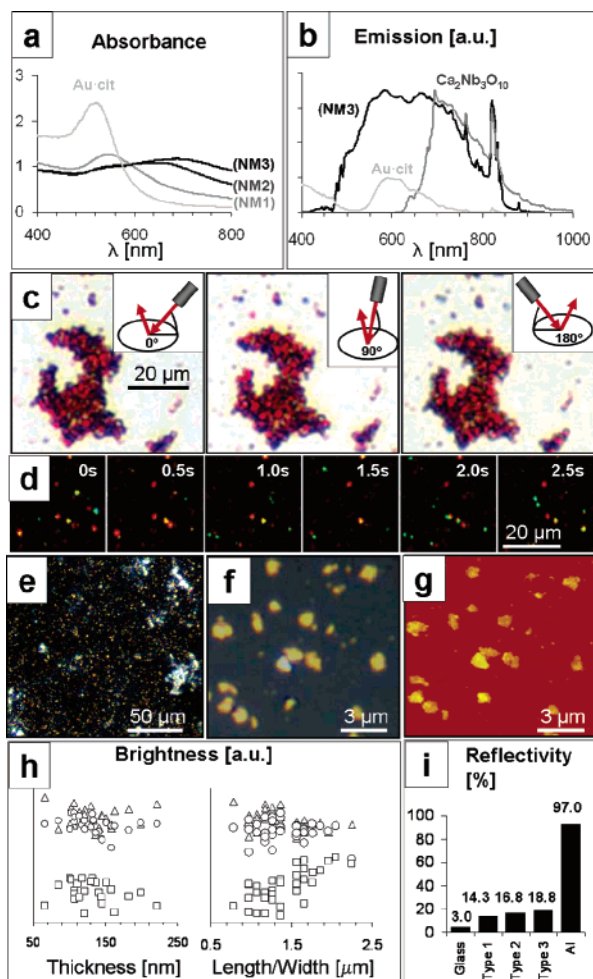


**Figure 2.** (a) Absorption spectra of NMs 1–3 and citrate gold particles in water. (b) Synchronous scan emission spectra for NMs 3 in ethanol, citrate-coated gold nanoparticles ( $\text{H}_2\text{O}$ ), and  $\text{Ca}_2\text{Nb}_3\text{O}_{10}$  plates in THF (narrow peaks are instrument artifacts). (c) Light reflection by  $\sim 100$  type 3 NMs under illumination with laser light (654 nm) directed at the sample in the indicated directions (10X objective, NA = 0.25). (d) Micrographs of NMs 3 suspended in ethanol/glycerol (1:1 v/v) under illumination with green (532 nm) and red (654 nm) laser light. Pictures were taken in 0.5 s intervals. (e) Optical micrographs (10 $\times$  objective, NA 0.25) of type 3 NMs under Hg light illumination (reflected light). (f) Micrograph (100 $\times$  objective, NA 0.95) and AFM scan (g) of individual NMs 3 on a glass slide. (h) Plots of the reflected light intensity for NMs 3 on glass as a function of particle thickness and lateral size. Triangles (650 nm), circles (510 nm), and squares (440 nm) indicate emitted wavelengths. (i) Comparison of the reflectivity of NMs (%).

orientations, NMs either remain dark or reflect green or red light, or both, which leads to a yellow appearance. Some of the NMs appear light blue due to an effect that we currently do not understand. Overall, this experiment demonstrates that the angular light reflection properties of the particles are retained in solution, and it suggests a potential of NMs for high-resolution color displays.

To determine structure–property relationships in the nanoparticle mirrors, brightness and topology of individual type 3 particles were measured separately with optical and atomic force microscopes (Figure 2f,g). The analysis of these data (Figure 2h) shows that the reflectivity of the structures is smaller for blue light (440 nm) than for yellow (510 nm) or red (650 nm) light. This behavior,

which is due to the plasmon absorption of the gold nanoparticles, is similar to what is observed for the particle dispersion (Figure 2b). The intrinsic reflectivity also appears to be independent of the thickness and lateral sizes of the NMs, except for blue light ( $\lambda = 440$  nm), for which a trend of increasing particle brightness with increasing lateral size is observed. The small influence of the NM thickness on the reflectivity indicates that light only penetrates the top portion of these structures. This agrees well with the high optical absorption coefficient of bulk gold ( $1.5 \times 10^6 \text{ cm}^{-1}$ ),<sup>11</sup> which corresponds to a light penetration depth of  $\sim 10$  nm. Overall, the optical properties of NMs 1 and 2 are similar to those of 3 except that the overall reflectivities are smaller (Figure 2i). By comparing the brightness of NMs illuminated along the surface normal with that of glass and polished aluminum one can estimate that the NM reflectivities are between 14.3 and 18.8%. The relatively small values are expected considering the surface roughness of these structures.

In conclusion, we have demonstrated a chemical synthesis of microscale particles with mirror-like properties. This bottom-up approach is complementary to lithography-based methods in that it allows the fabrication of  $>10^{14}$  micromirrors using only a few synthetic steps and inexpensive starting materials. The method might enable new applications of micro-sized mirrors as optical probes to investigate flow dynamics or as reflective components in high-resolution displays. Integration of these micromirrors into silicon-based optics devices might be possible using fluidic assembly.<sup>12</sup> Further studies on the angle-dependent light emission of nanoparticle mirrors and their applications are underway.

**Acknowledgment.** We thank Dr. Susan Kauzlarich for providing furnaces, and Dr. Ting Guo for helpful discussions. J.Y.K. thanks the Tyco Electronics Corporation for a summer fellowship. This work was supported by a grant from the National Science Foundation.

**Supporting Information Available:** Full synthetic details, SEM micrographs of type 3 NMs, polarized optical micrographs of type 3 NMs and of ZnO particles, and a movie showing light reflection by type 3 NMs suspended in ethanol/glycerol. This material is available free of charge via the Internet at <http://pubs.acs.org>.

## References

- Shroff, Y.; Chen, Y. J.; Oldham, W. *J. Vac. Sci. Technol. B* **2001**, *19* (6), 2412–2415.
- Singh-Gasson, S.; Green, R. D.; Yue, Y. J.; Nelson, C.; Blattner, F.; Sussman, M. R.; Cerrina, F. *Nat. Biotechnol.* **1999**, *17* (10), 974–978.
- Lin, L. Y.; Goldstein, E. L.; Tkach, R. W. *IEEE Photon. Technol. Lett.* **1998**, *10* (4), 525–527.
- Jain, A.; Qu, H. W.; Todd, S.; Xie, H. K. *Sens. Actuators, A* **2005**, *122* (1), 9–15.
- Van Kessel, P. F.; Hornbeck, L. J.; Meier, R. E.; Douglass, M. R. *Proc. IEEE* **1998**, *86* (8), 1687–1704.
- Kim, J. Y.; Osterloh, F. E. *J. Am. Chem. Soc.* **2005**, *127* (29), 10152–10153.
- Kim, J. Y.; Osterloh, F. E.; Hiramoto, H.; Dumas, R. K.; Liu, K. *J. Phys. Chem. B* **2005**, *109* (22), 11151–11157.
- Osterloh, F. E. *J. Am. Chem. Soc.* **2002**, *124* (22), 6248–6249.
- Kim, J. Y.; Hiramoto, H.; Osterloh, F. E. *J. Am. Chem. Soc.* **2005**, *127* (44), 15556–15561.
- Lyklema, J. *Fundamentals of Interface and Colloid Science*; Academic Press: San Diego, CA, 2000; p 3.
- Weaver, J. H.; Krafka, C.; Lynch, D. W.; Koch, E. E. *Optical Properties of Metals*; Fachinformationszentrum Energie Physik Mathematik GmbH: Karlsruhe, Germany, 1981; Vols. 18–22, p v.
- Srinivasan, U.; Helmbrecht, M. A.; Rembe, C.; Muller, R. S.; Howe, R. T. *IEEE J. Selected Topics In Quantum Electronics* **2002**, *8* (1), 4–11.

JA057958K